Conformation of gelatin chains in aqueous solutions: 1. A light and small-angle neutron scattering study

I. Pezron, M. Djabourov* and J. Leblond
Laboratoire de Physique Thermique, CNRS URA 857, ESPCI, 10 rue Vauquelin, 75231 Paris Cedex 05, France
(Received 1 August 1990; revised 8 October 1990; accepted 10 October 1990)

Gelatin solutions in dilute and semi-dilute regimes were characterized by using light and small-angle neutron scattering techniques. Absolute intensity measurements allowed us to evaluate the molecular parameters of these protein chains (radius of gyration, persistence length, cross-section, mass per unit length) and to determine the quality of the solvent (0.1 M NaCl solutions in H_2O or D_2O at pH = 7). The classical model of worm-like chains was adopted for the theoretical interpretation of chain conformation in the sol state ($T = 50$ °C) with a persistence length of about 20 Å. In semi-dilute solutions the correlation length was measured for different concentrations. Agreement was found with the scaling laws, although the description is not totally satisfactory: non-trivial scattering effects are detected in both static and dynamic light scattering experiments, which can be attributed to the presence of inhomogeneities having a different local density. Their apparent radius of gyration is of the order of several hundred angstroms. The nature and extension of these inhomogeneities are discussed.

(Keywords: conformation; gelatin; solution; light scattering; small-angle neutron scattering; characterization; modelling)

INTRODUCTION

Gelatin is a biopolymer obtained from denaturation of collagen, the most abundant protein in mammals. At temperatures above 37 °C, the gelatin solutions are in the sol state. Provided that the gelatin concentration is high enough (around 1%, depending on the gelatin composition), solutions change into gels when they are cooled to room temperature: an infinite network connecting all the chains throughout the solvent then appears.

Gel properties have been extensively studied, but only little attention has been paid so far to the structural characteristics of gelatin chains in solutions, particularly in the concentrated regime, where the gels are formed. During the last decade, powerful radiation sources, such as synchrotron radiation and neutron sources, have become available to experimentalists working on condensed matter. These facilities now allow characterization of a polymeric or a colloidal solution on spatial scales between 10 and 1000 Å. At the same time, considerable theoretical progress has been made in understanding the structure of polymeric solutions in different ranges of concentration based on the analysis of scaling laws[1-4]. In order to establish a valid test of the theoretical models, investigations were undertaken with samples of variable molecular weights, with different solvents and various polymer concentrations; in some cases, isotopic substitutions have been made. Such experiments, indeed, lead to improved knowledge of the structural and thermodynamic properties of dilute and semi-dilute polymeric solutions, but they only concern a limited number of 'model' samples.

Light scattering (LS) and small-angle X-ray scattering (SAXS) techniques[1] have been applied mainly to natural polymer solutions in the dilute regime. Molecular parameters such as radii of gyration, molecular weights, virial coefficients and sometimes persistence lengths have been determined for polysaccharides, globular or elongated proteins and nucleic acids. In the case of gelatin, in an early LS work, Boedtker and Doty[5] have reported measurements of the radii of gyration of the chains for different molecular-weight distributions. The effects of salt and pH on chain expansion have also been examined. The authors concluded that the model of ideal chains applies to the conformation of gelatin chains.

In order to improve knowledge of the gelatin process, an investigation of the structure of aqueous gelatin solutions has been considered. Using two complementary techniques, LS and small-angle neutron scattering (SANS), we were able to extend the range of scattering vectors from 8×10^{-4} to 3×10^{-1} Å^{-1}, which allowed us to characterize the gelatin solutions on a wide spatial scale and in different regimes of concentration. Besides, a quasi-elastic light scattering study was undertaken, which is reported in the accompanying paper[6]. We were then able to follow the modifications arising from gelation. This system, which is also being studied by several other techniques in our laboratory (rheology, polarimetry, electron microscopy)[7,8], provides a comprehensive picture of gelation mechanisms.

In this study we have determined the characteristic molecular parameters of the chains in the sol state and examined whether the existing statistical models can account for the measurements, for various gelatin concentrations. Comparisons were made with other systems of linear polymers in solution.

* To whom correspondence should be addressed

0032-3861/91/173201-10

EXPERIMENTAL

Materials

The gelatin sample is a lime processed ossein extract (Rousselot gelatin, a photographic grade type), kindly supplied by Sanofi-Bio-Industries. The molecular-weight distribution, obtained by gel permeation chromatography, is shown in *Figure 1*: the major component is centred around $M = 10^5$ g mol^{-1} (collagen single chain) and the distribution is characterized by a polydispersity index $M_w/M_n = 2.3$ with $M_w = 1.9 \times 10^5$ g mol^{-1}. The isoelectric point for this sample is pH = 5.

Gelatin solutions were prepared using the following procedure. First, dry gelatin granules were allowed to swell for 12 h at $T = 4$°C in a 0.1 M NaCl aqueous solution. A small amount of sodium azide was added to prevent bacterial contamination. The mixture was then heated to $T = 50$°C and stirred for 1 h. The pH was adjusted to pH = 7 by adding a few drops of sodium hydroxide solution. Concentration was measured by weighing the solutions and correcting for the amount of water adsorbed on the granules (10% by weight). In LS experiments, demineralized water (Millipore Super Q) was used and the samples were filtered with 0.45 μm Millipore filters. After filtering, the final concentration was checked by optical rotation measurements (the losses by filtration were negligible). In SANS experiments, heavy water D_2O (99.8% pure) was used instead of water, to obtain better contrast and less background intensity (the large incoherent background is mainly due to the scattering of protons). All concentrations are expressed in grams of gelatin per unit volume of the solution (g cm^{-3}).

Techniques

SANS experiments were performed on the PACE spectrometer at Laboratoire Léon Brillouin (Laboratoire Commun CEA-CNRS, Saclay, France). Using two different configurations, $\lambda = 12.3$ Å and $\lambda = 5.5$ Å, the scattering vector range covered was:

$$5 \times 10^{-3} < q < 3 \times 10^{-1} \text{ Å}^{-1}$$

We recall that the scattering vector q is defined by

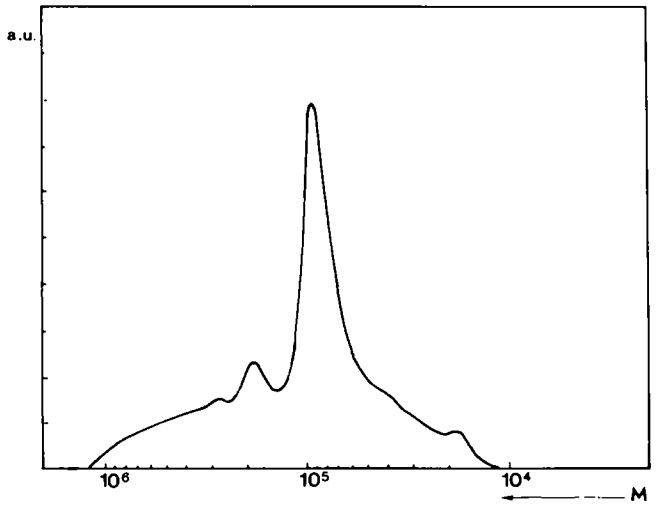

Figure 1 Molecular-weight distribution of the gelatin sample, obtained by gel permeation chromatography on a Sepharose CL4B column and measured by absorbance at $\lambda = 230$ nm (by courtesy of Sanofi-Bio-Industries)

$q = (4\pi/\lambda)\sin(\theta/2)$, where λ is the neutron wavelength and θ the scattering angle.

Experiments were performed using quartz cells thermostated at 50°C, with an optical path of 5 mm and counting times ranging from 3 to 10 h. The measured intensities were corrected for the background signal of the solvent. The contribution due to the incoherent background arising from protons of the gelatin chain was estimated by measuring the scattered intensity of an H_2O/D_2O mixture containing the same H/D ratio as the gelatin solutions.

Absolute intensities (expressed in cm^{-1}) were obtained by normalization to the isotropic scattering intensity of protonated water, H_2O. The contrast of scattering length, which appears as a constant factor in the expression for the scattering function of the solution (see for instance equation (11)) is defined as[9]:

$$(\rho - \rho_0)^2 = \left(\frac{\sum f}{v} - \frac{\sum f_0}{v_0}\right)^2 \qquad (1)$$

Here ρ and ρ_0 are, respectively, the scattering-length density of the polymer and of the solvent, $\sum f$ and $\sum f_0$ represent the total scattering length of a polymer unit and of the solvent molecule, and v and v_0 are the corresponding volumes. We considered as a typical gelatin unit the sequence Gly-Pro-X, X having an average composition of the remaining residues calculated from a standard composition of gelatin extracted from bones[10]. The molecular volume of this sequence is 306 Å^3 and the corresponding mass 265 g mol^{-1}. The contrast factor is found equal to $(\rho - \rho_0)^2 = 1.79 \times 10^{21}$ cm^{-4}.

LS experiments were performed with a vertically polarized He Ne laser beam, of wavelength $\lambda_0 = 6328$ Å. The scattered intensity was detected for scattering angles ranging from 30° to 150°. The corresponding scattering vector range is:

$$6.8 \times 10^{-4} < q < 2.5 \times 10^{-3} \text{ Å}^{-1}$$

The data were corrected for solvent scattering and variation of the scattering volume at different angles. Absolute intensities were obtained by comparison with the scattering of benzene. The contrast factor is related to the increment of refractive index dn/dc of the solution by the relation:

$$(\rho - \rho_0)^2 = \frac{(2\pi)^2}{\lambda_0^4 N_A} n_0^2 \left(\frac{dn}{dc}\right)^2 d^2 \qquad (2)$$

Here dn/dc was measured for gelatin solutions and found to be $dn/dc = 0.18$ ml g^{-1}; d, the gelatin density, is 1.44 g cm^{-3}; for aqueous solutions, n_0 is the refractive index of water (1.33); N_A is the Avogadro number.

Knowing the absolute intensities for both techniques allowed us to gather data from different scattering vector ranges in one, almost continuous, plot.

THEORETICAL BACKGROUND

The dilute regime

Structure factor of an isolated chain in solution. Scattering techniques are the only tools which give direct information on the conformational statistics of polymer coils. The conformation of a single chain in solution depends on both short- and long-range interactions[1]. *Short-range interactions* between neighbouring monomers

originate from steric hindrance restricting the motion of molecular groups about chemical bonds and provide local rigidity to the chain. Short-range interactions may also be due to electrostatic effects, in polyelectrolyte solutions. However, these effects are screened in high-salt conditions. Rigidity is expressed through the value of the statistical unit length b, defined for instance in Kuhn's model[11]. Monomers that are far apart along the chain may come close to each other and then undergo *long-range interactions*, which are governed by excluded-volume effects. The chain conformation depends on the balance between monomer monomer and monomer - solvent interactions and is characterized by the radius of gyration R_g, which is the mean-square distance of all monomers to the centre of gravity of the polymer.

The normalized scattering function of a single chain is related to the conformational statistics of its monomers through the relation:

$$P_1(q) = \frac{1}{N^2} \sum_{i=1}^{N} \sum_{j=1}^{N} \langle \exp[i\mathbf{q}(\mathbf{r}_i - \mathbf{r}_j)] \rangle \qquad (3)$$

where $P_1(q)$ is the structure factor of the single chain and N is the number of statistical units. Expression (3) can be simplified, by making assumptions about the conformation of the chains in different ranges of scattering vectors:

(a) In the Guinier range ($q < R_g^{-1}$) the scattering function can be approximated by:

$$P_1(q) \approx 1 - q^2 R_g^2/3 \qquad (4)$$

Using this relation, one can determine the radius of gyration from LS experiments (Zimm plot).

(b) In the intermediate range of scattering vectors ($R_g^{-1} < q < b^{-1}$) the structure factor is directly related to the statistical distribution of elementary units. Two cases are generally considered, the Gaussian coil and the swollen coil. A Gaussian coil is characterized by equal monomer -monomer and monomer - solvent interactions (theta solvent). In a good solvent, the different interactions result in a repulsion between monomers: the coil swells. In the range $q < b^{-1}$, Debye[12] obtained the following expression for a Gaussian conformation:

$$P_1(x) = \frac{2(e^{-x} + x - 1)}{x^2} \qquad (5)$$

where $x = q^2 R_g^2$. For $q \to \infty$ the following simplified expression is derived:

$$P_1(q) \approx \frac{2}{q^2 R_g^2} \qquad (6)$$

Within 5% error, this characteristic asymptotic behaviour is reached at $qR_g = 5$. The radius of gyration R_g is related to the molecular weight M, to the weight per unit length M_1 and to the statistical unit b, through the relation:

$$R_g^2 = \frac{bM}{6M_1} \qquad (7)$$

For swollen coils, scaling laws[4] and computer simulations have shown that for $q \to \infty$:

$$P_1(q) \sim q^{-1/\nu} \qquad (8)$$

where ν is the excluded-volume parameter; $\nu = 3/5$ in a good solvent. Strictly speaking, this prediction is valid for infinitely long chains. Experimentally, to distinguish between two asymptotic behaviours requires a large enough range $R_g^{-1} < q < b^{-1}$ and very precise measurements[13]. Practically, the intermediate scattering range starts beyond $qR_g = 3$.

(c) For $q > b^{-1}$ the local rigidity and the cross-section of the chain have an influence on its scattering function. The structure factor of an infinitely thin worm-like chain has been calculated by Kratky and Porod[14]. For $q \to \infty$ and $N \to \infty$:

$$P_1(q) \approx \frac{\pi M_1}{qM} \qquad (9)$$

This is the scattering from a rod-like particle with a negligible thickness. When the cross-section is taken into account an approximate relation can be obtained:

$$P_1(q) \approx \frac{\pi M_1}{qM} \exp\left(-\frac{q^2 R_c^2}{2}\right) \qquad (10)$$

where R_c is the radius of gyration of the cross-section. The correction term is important in the range $b^{-1} \ll q < R_c^{-1}$.

Scattering from a dilute solution of chains

(a) *A monodisperse solution.* So far, only the scattering of single particles has been treated. For solutions containing n identical macromolecules, not only the single-particle scattering has to be considered, but interparticle interference effects must also be taken into account. Indeed, the scattering function of chains in dilute solutions has been calculated by Zimm[15] in the presence of interference effects:

$$P(q) = kcM[P_1(q) - 2A_2cMP_1(q)^2] \qquad (11)$$

Here $P(q)$ is the scattering cross-section per unit irradiated volume, M is the molecular weight of the chains, c is the concentration of chains (mass per unit volume), A_2 is the second virial coefficient, $k = (\rho - \rho_0)^2/d^2$ is a constant, which depends on the scattering technique, and $(\rho - \rho_0)^2$ is the contrast factor, defined in equation (2). In the Guinier range of scattering vectors, equation (11) becomes:

$$\frac{kc}{P(q)} = \frac{1}{M}\left(1 + \frac{q^2 R_g^2}{3}\right) + 2A_2c \qquad (12)$$

Interparticle repulsive effects lead to a decrease of the scattered intensity with increasing concentration at small angles ($q \to 0$).

(b) *A polydisperse solution.* A macromolecular, and especially a biopolymer, solution usually contains chains of different lengths. When the polydispersity is known from other techniques, like gel permeation chromatography, the mass distribution function can be introduced for correction of the scattering function[1]. So, the z-averages of the structure factor and of the mean-square radius of gyration can be computed. The inverse operation, which consists of deriving the molecular-weight distribution from the experimental data, needs for practical use an extremely high accuracy of the measurements (see below). On the other hand, an approximate expression for the structure factor of single chains can be obtained by introducing a standard shape of molecular-weight distribution[16] like, for instance, the Schulz distribution[17], where polydispersity is accounted for by a parameter U

that characterizes the width of the mass distribution:

$$U = M_w/M_n - 1$$

M_w/M_n is the polydispersity index. In the case of Gaussian coils, the following normalized scattering function is obtained[1]:

$$\langle P_1(q)\rangle_z = \frac{2[(1+Uy)^{-1/U} + y - 1]}{(1+U)y^2} \qquad (13)$$

where

$$y = \frac{\langle R_g^2\rangle_z q^2}{1+2U}$$

The asymptotic q^{-2} behaviour appears in the intermediate range of scattering vectors, as for a monodisperse solution of coils.

In a dilute polydisperse solution, the Zimm equation (12) has to be rewritten by introducing the average values of the radius of gyration and of the molecular weight and by taking into account the polymer–solvent interactions. One has:

$$\frac{kc}{P(q)} = \frac{1}{M_w}\left(1 + \frac{q^2\langle R_g^2\rangle_z}{3}\right) + 2A_2c \qquad (14)$$

The semi-dilute regime in good solvents

When polymer concentration in solution is increased above a certain limit c^*, chains interpenetrate each other. The overlap concentration c^* for a monodisperse solution can be deduced from the values of the molecular weight and of the radius of gyration of the chains. This limit determines the crossover between the dilute and semi-dilute regimes, which occurs when the concentration of the solution is comparable to the local concentration inside a single coil. Theoretical studies worked out by Edwards[18], and more recently by des Cloizeaux[19], Daoud *et al.*[2] and de Gennes[4], predict that the structural properties of the solutions for $c > c^*$ can be expressed as a function of one fundamental parameter, ξ, the screening length. In a good solvent ξ is the average mesh size of the transient network of chains. De Gennes[4] suggested that the pair-correlation function should follow an Ornstein–Zernike law. This assumption leads to a Lorentzian form of the scattering function, in the range $q < \xi^{-1}$:

$$P(q) = \frac{P(0)}{1 + q^2\xi^2} \qquad (15)$$

Plotting the inverse of the scattered intensity as a function of the square of q, a straight line should be observed, whose slope is ξ^2. According to the scaling laws, ξ varies with the concentration as:

$$\xi = R_g\left(\frac{c}{c^*}\right)^{\nu/(1-3\nu)} \qquad (16)$$

where ν is the excluded-volume parameter. In the range $q > \xi^{-1}$, the scattering function is identical to a dilute solution of chains.

EXPERIMENTAL RESULTS AND ANALYSIS

In this section we shall examine the light and neutron scattering from gelatin solutions of different concentrations. The data are analysed within the general theoretical framework that was introduced in the previous section. The aim of this analysis is:

(i) to provide a full characterization of the conformation of the individual chains (radius of gyration, persistence length, cross-section and mass per unit length) and of the quality of the solvent (virial coefficient); and

(ii) to describe the supramolecular arrangements in the entangled solutions, above the overlap concentration c^*.

This study was a necessary step before the investigation of the gel structure. Modifications of the scattering spectra due to gel formation will be examined in a forthcoming article.

Figure 2 shows the scattering curves from gelatin solutions of various concentrations increasing from 0.2% to 5%. Absolute intensities I, normalized by concentration, are plotted on a double logarithmic scale as a function of the scattering vector q. The values obtained by light and neutron scattering are plotted. Heavy water D_2O is used in SANS experiments and hydrogenated water for LS measurements, both solutions being 0.1 M NaCl at 'pH = 7'. Temperature was fixed at $T = 50°C$. The scattering vector range covered three decades, from 5×10^{-4} to 3×10^{-1} Å^{-1}, while the amplitudes of the scattered intensities also varied over three decades, in particular for the most dilute sample, justifying a double logarithmic representation of I *versus* q. The experimental facilities did not allow measurements in the range $2 \times 10^{-3} < q < 5 \times 10^{-3}$ Å^{-1}. Concentration effects due to interparticle interferences only occur at small angles and they become more pronounced on increasing the number of macromolecules. At higher scattering vectors, $q > 2 \times 10^{-2}$ Å^{-1}, the various plots are almost indistinguishable. The different plots in *Figure 2* correspond to the dilute and semi-dilute regimes, the limit between the two being around $c^* \approx 0.5\%$ (see below).

Chain conformation in dilute solutions

The LS and SANS measurements. The data correspond to the concentration $c = 0.2\%$ in *Figure 2*. The plot covers three ranges of scattering vectors, the Guinier range, the intermediate range and the asymptotic range.

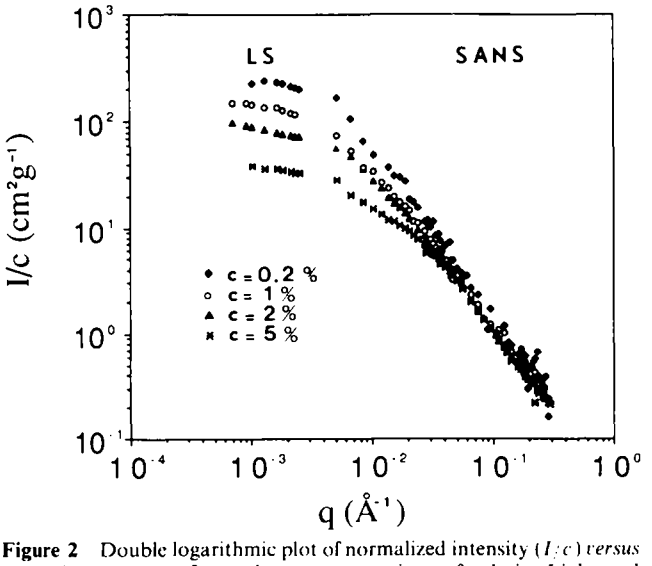

Figure 2 Double logarithmic plot of normalized intensity (I/c) *versus* scattering vector q, for various concentrations of gelatin. Light and small-angle neutron scattering data are gathered. Gelatin solutions are 0.1 M NaCl, at pH = 7 and $T = 50°C$, in either H_2O or D_2O solution

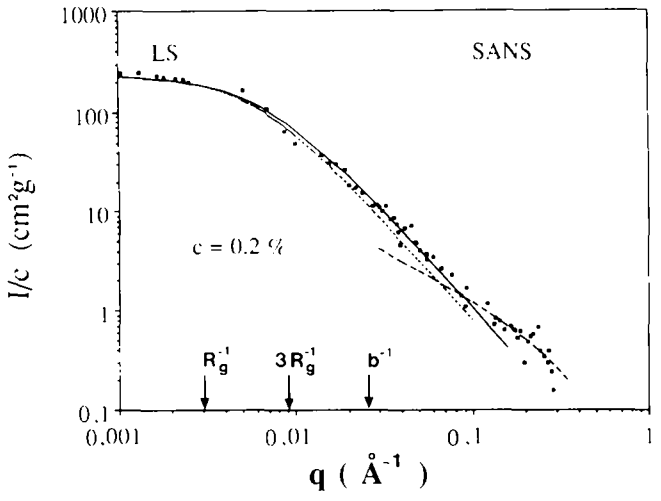

Figure 3 Absolute normalized intensity scattered by a gelatin solution of $c = 0.2\%$. The experimental data are fitted using equation (11) in Guinier and intermediate scattering vector ranges: the dotted curve assumes a Schulz distribution of the molecular weight, with a polydispersity index of 2.3, and the full curve was calculated with the distribution given in *Figure 1*. Equation (10) is used in the asymptotic range (broken curve). The inverses of the average radius of gyration R_g and of the statistical unit b are also indicated. The numerical values for the parameters are gathered in *Table 1*

From a separate LS experiment[20] we have determined the z-average radius of gyration of the chains at infinite dilution and found $R_g = 350 \pm 40$ Å. The intermediate range, $3R_g^{-1} < q < b^{-1}$, where both effects of polydispersity and swelling occur, starts above $q = 9 \times 10^{-3}$ Å^{-1}. We first attempted to fit the data, in both the Guinier and the intermediate ranges, by using the scattering function of polydisperse Gaussian coils, for which we have an analytical form (equations (13) and (14)). The best fit is shown on *Figure 3* with the following values of the parameters:

$M_w = 1.9 \times 10^5$ g mol^{-1} $\quad A_2 = 3 \times 10^{-4}$ mol ml g^{-2}

$(\langle R_g^2 \rangle_z)^{1/2} = 330$ Å $\quad U = 1.3$

The weight-average molecular weight and the polydispersity index were assumed from gel permeation chromatographic measurements and the virial coefficient was determined from the Zimm plots[20]. One can see that approximate agreement is observed up to a scattering vector of 10^{-1} Å^{-1} (dotted curve). The next step of this analysis is to justify how far the intermediate range should extend. To this end, one has to determine the persistence length of the chain.

A close examination of the outer part of the curve (for instance, $q > 5 \times 10^{-2}$ Å^{-1}) enables one to derive the local parameters of the chain. Assuming equation (10) to be valid and using absolute intensity measurements, by plotting $\log(qI/c)$ *versus* q^2, one can derive simultaneously the cross-section of the chain R_c and the mass per unit length M_1:

$$\log\left(\frac{qI}{c}\right) = -\frac{R_c^2 q^2}{2} + \log\left(\frac{(\rho - \rho_0)^2}{d^2} \cdot \pi M_1\right) \quad (17)$$

From the slope of the linear part of the plot, as shown in *Figure 4*, one can deduce $R_c = (3.2 \pm 1)$ Å. Such a value is in agreement with the lateral extension of a collgen single chain derived from crystallographic data: $R_c = 2.5$ Å. For comparison, $R_c = 3.1$ Å for fully deuterated polystyrene[14]. One also derives $M_1 = (28 \pm 8)$ g mol^{-1} Å^{-1} when absolute intensity is considered. The mass per unit length can be calculated from the molecular composition of the chain: the average mass per three residues being 265 g mol^{-1} and the length of a peptide bond being of the order of 3–3.5 Å, this gives a value for M_1 close to our experimental result (29.4 25.2 g mol^{-1} Å^{-1}).

In order to derive the statistical unit b of the chain, one has to find the scattering vector q^* corresponding to the transition from coil to rod-like behaviour. This can be done by using the so-called Kratky representation. Indeed, when one plots $q^2(I/c)\exp(q^2R_c^2/2)$ *versus* q according to equation (10), one should observe, at large values of q, either a linear part with a slope proportional to M_1 for a rod-like behaviour or, according to equation (6), a horizontal line. The scattering from a rod-like particle is shown with a broken line. The intersection of the two scattering regimes occurs for an approximate value q^* such as $q^*R_c \approx 1$ and:

$$q^*b \approx 12/\pi \quad (18)$$

We find $0.08 < q^* < 0.1$ Å^{-1}. So, the statistical unit b is around $b = (40 \pm 5)$ Å. It should be stressed that the asymptotic range of q vectors, $q > b^{-1}$, holds for $q > 2.5 \times 10^{-2}$ Å^{-1}, which indeed corresponds to the range where equation (10) was found to be valid. The persistence length, which by definition is $l = b/2$, is equal to $l = (20 \pm 3)$ Å.

One may turn back to the whole scattering curve and try to fit the data by using the exact molecular-weight distribution, known from chromatography. We assume a Gaussian chain conformation and take the numerical values of the statistical unit b, of the mass per unit length M_1 and of the virial coefficient A_2 previously derived (equations (5), (7) and (11)). Thus[1]:

$$\langle P_1(q) \rangle_z = \frac{1}{M_w} \int_0^\infty P_1(M) M m(M)\, dM$$

where $m(M)$ is the mass distribution function taken from *Figure 1*.

The plot is shown with a full curve in *Figure 3*: one can see now the very good agreement between the experimental data and the calculated values. The discrepancy that appeared with the first fit (dotted curve) was probably due to the inadequacy of the Schulz equation[17] to describe the molecular-weight distribution of our

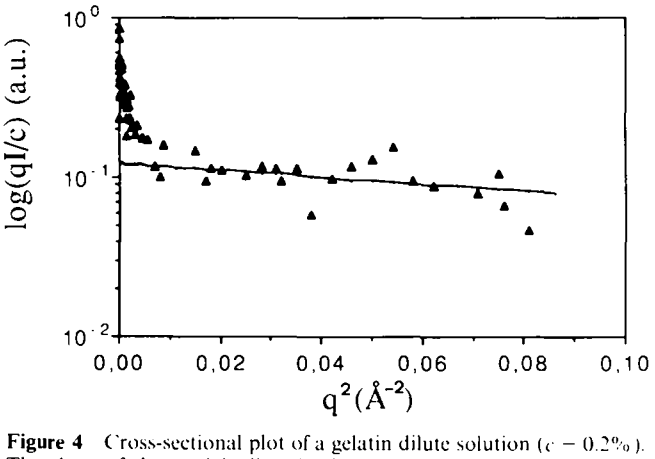

Figure 4 Cross-sectional plot of a gelatin dilute solution ($c = 0.2\%$). The slope of the straight line, in the asymptotic range of scattering vectors, gives $R_c = (3.2 \pm 1)$ Å

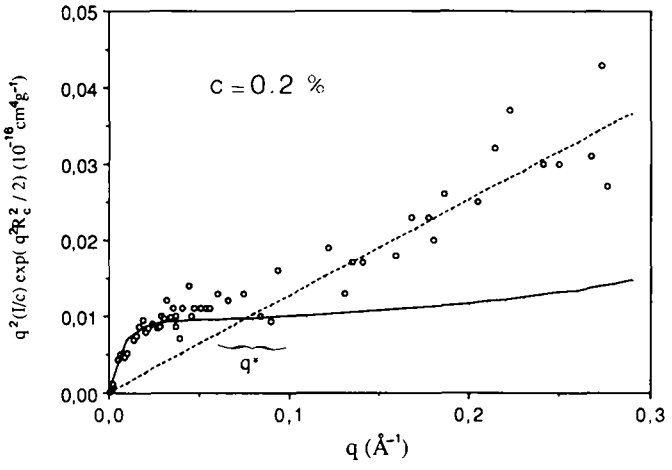

Figure 5 Kratky diagram of a dilute gelatin solution, $c = 0.2\%$: the full curve represents the Gaussian chain (equation (11), molecular-weight distribution from *Figure 1*) and the broken line is the asymptotic behaviour of an infinite rod-like chain with a cross-section R_c (equation (10)). The intersection of the two curves indicates the approximate value for q^*

Table 1 Characteristic parameters of the gelatin chains deduced from the scattering experiments in the dilute regime

Parameters	Numerical values
$(\langle R_g^2 \rangle_z)^{1/2}$	350 ± 40 Å
M_w	$(1.9 \pm 0.1) \times 10^5$ g mol^{-1}
M_w/M_n	2.3
A_2	$(3 \pm 1) \times 10^{-4}$ mol ml g^{-2}
b	(40 ± 5) Å
R_c	(3.2 ± 1) Å
M_l	(28 ± 8) g mol^{-1} Å^{-1}

sample. The calculated curve is also shown in *Figure 5*, demonstrating the transition from coil to rod-like behaviour.

Discussion. The characteristic parameters of our gelatin sample are summarized in *Table 1* with the corresponding errors. The overall picture that arises from this investigation of dilute aqueous solutions is in agreement with the assumption that this protein adopts in the sol state the conformation of random coils. This conclusion is mainly based on the detailed analysis of the scattering spectra over a wide range of q vectors. The macromolecule is correctly dissolved in either H_2O or D_2O solvents containing 0.1 M NaCl. These solvents are characterized by a high proportion of salt, whose effect is to shield the protein electrostatic charges[21]. As a first approximation[22] one can refer to the general theories of neutral polymer solutions and calculate an effective value of the Flory parameter χ, deduced from A_2. One finds $0.48 < \chi < 0.49$. Good solvents (polystyrene in carbon disulphide or in benzene) have χ parameters of the order of 0.40 to 0.45. The solvent quality for this system appears to be slightly lower, as can be expected for water-soluble polymers where intrachain hydrogen bonds may prevent maximum swelling.

One can make some further comments. When dealing with flexible coils in good solvent solutions, the classical picture of Gaussian coils is incorrect: the main difference in the scattering function appears in the intermediate scattering vector range, where the power law given by equation (8) should be observed instead of equation (6). We were not able to detect such an effect. Indeed, as has been clearly demonstrated by Rawiso *et al.*[13], using polystyrene, one needs high-molecular-weight samples of rather flexible polymers in order to observe the scaling-law behaviour of swollen coils. Then, the range:

$$R_g^{-1} \ll q \ll b^{-1}$$

would be as large as possible. For low or moderate molecular weights, no distinction can be made between the two models because the intermediate q range is reduced too much. Besides, when polydisperse solutions are considered, the inequalities above are even more difficult to fulfil. Then, examining *Figure 3* again one can see that the intermediate range extending from:

$$3(\langle R_g^2 \rangle_z)^{-1/2} < q < b^{-1}$$

is indeed limited and the experimental data are not accurate enough. One might expect to improve the analysis by using narrower molecular-weight distributions, but for a gelatin sample the average molecular weight can only decrease (by fractionating the sample).

Finally, we wish to stress the order of magnitude of the persistence length. It appears to be around 20 Å. This value is characteristic of a rather flexible chain. It corresponds to six polypeptide units along the chain or two sequences of the type Gly–Pro X. The abundance of the glycine residue (one-third of the residues) may be responsible for the flexibility of the chain. By comparison, flexible polymers such as polystyrene or poly(vinyl alcohol) have a persistence length of about 10 Å. A rigid polymer, like cellulose tricarbanilate, has a persistence length of 110 Å[23]. The local rigidity of the chain is likely to be an important factor in determining the rate and the amount of helical formation and association during gelation. It should be interesting too, for instance, to correlate the persistence length of the chains and the length of the junctions in the gel: indeed, in the case of agarose[24] and of κ-carrageenans[25], long helicoidal sequences (1000 Å) are formed from these very rigid chains.

Structure of semi-dilute solutions

We have investigated the scattering of semi-dilute solutions by varying the gelatin concentration: molecular weight, temperature and solvent are the same as in the previous study. The experimental data were shown in *Figure 2*. The measurements that are considered here are the three curves corresponding to concentrations 1%, 2% and 5%. According to theoretical predictions, the structure factors of solutions in good solvents are expected to exhibit a Lorentzian behaviour (equation (15)) in the scattering range $R_g^{-1} < q < b^{-1}$. So, we have plotted in *Figure 6* the inverse scattered intensities, $I^{-1}(q)$ *versus* q^2 for the three gelatin solutions, in the range of scattering vectors $5 \times 10^{-3} < q < 5 \times 10^{-2}$ Å^{-1}. A linear part is indeed observed approximately in the range $1.5 \times 10^{-2} < q < 5 \times 10^{-2}$ Å^{-1}. However, at lower scattering vectors, $q < 1.5 \times 10^{-2}$ Å^{-1}, a deviation from the Lorentzian shape appears, which is an excess scattering with respect to the linear law. We analyse separately these two ranges of scattering vectors.

First, we shall make the assumption that the linear part of each plot reflects, with no perturbation, the entangled regime, so that the correlation length can be

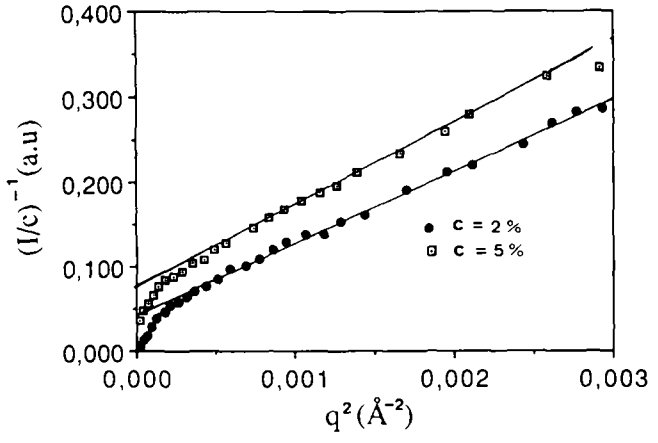

Figure 6 Inverse scattered intensities $(I/c)^{-1}$ *versus* q^2 for semi-dilute gelatin solutions ($5 \times 10^{-3} < q < 5 \times 10^{-2}$ Å^{-1}) of concentrations 2% and 5%. In the range of scattering vectors $1.5 \times 10^{-2} < q < 5 \times 10^{-2}$ Å^{-1} a linear dependence is observed whose slope allows one to calculate ξ. The values extrapolated to the vertical axis determine the amplitude of the Lorentzian component, $I_{Lorentz}(0)$. At small q vectors, an excess scattering appears (downwards curvature)

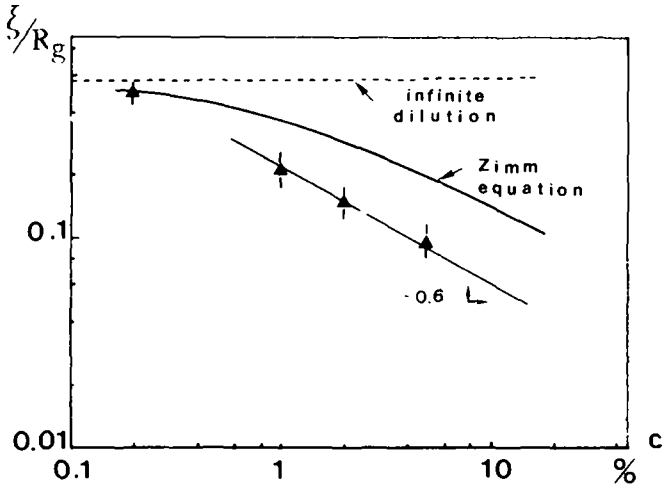

Figure 7 Concentration dependence of the screening length, illustrating the transition from dilute to semi-dilute regime. A power law with an exponent −0.6 is observed in the semi-dilute range. In the dilute range, ξ is the apparent screening length, which can be calculated from the Zimm equation (14). For infinite dilution one has $\xi/R_g \rightarrow 1/\sqrt{3}$ (see for instance ref. 31)

Table 2 Correlation lengths and sizes of inhomogeneities in the semi-dilute solutions

c (%)	ξ (Å)	a (Å)
1	70 ± 10	
2	51 ± 5	220
5	35 ± 3	135

deduced. Three values can be extracted, which are gathered in *Table 2*. The concentration dependence of the screening length is shown in *Figure 7*. By plotting both equations (14) and (15), the transition from dilute to semi-dilute regime is clearly illustrated. The concentration dependence of the screening length ξ is expected to follow a power law with an exponent of −0.75 for a good solvent, and −1 for a theta solvent. Although there are only a few data points, our experimental results suggest a rather smaller value, between −0.5 and −0.7. Such a value is consistent with the picture of a semi-dilute solution which does not display strong swelling effects. Indeed, Schaefer *et al.*[26,27] have undertaken an analysis based on a perturbation theory of the mean-field approximation, which applies to polymer solutions where excluded-volume effects are weak, but not absent. This regime was called by Schaefer[27] the *marginal regime*. The marginal regime is an intermediate state between a good solvent and a theta solvent, and it is observed in solutions of semi-flexible chains. With increasing concentration, the marginal regime starts from c^-, a value close to c^*, $c^- > c^*$, and extends to a c^+ value, which is $c^+ \approx (1 - 2\chi)$. In this concentration range, the ξ exponent should be close to −0.5. Our measurements are consistent with this interpretation ($c^+ \approx 5\%$).

We focus now on the excess intensity that appears at low angles. Excess intensities were clearly pointed out in *Figure 6*, where $(I)^{-1}$ was plotted *versus* q^2. By taking the numerical values for ξ given above, one can show on a double logarithmic plot of $I(q)$ the contribution of the Lorentzian component and the amount of excess scattering (*Figure 8*). Excess scattering has already been reported in a number of polymeric solutions[28,29] although others have been found in full agreement with the Lorentzian behaviour[30] (see next section). To account for the angular distribution of excess intensities, Kolberstein *et al.*[31] adapted the Debye Bueche[32] theory of scattering by a heterogeneous solid to the case of polymer solutions: contributions from long-range concentration fluctuations appear in inhomogeneous solutions, in addition to the scattering due to the uniform part. If the spatial scale of the density fluctuations due to inhomogeneities is large compared to the correlation length ξ, then the two contributions can be treated separately and added to calculate the total intensity:

$$I(q) = I_{Lorentz}(q) + I_{ex}(q) \qquad (19)$$

Debye and Bueche proposed to characterize the extensions of the inhomogeneities by a correlation function $\gamma(r)$

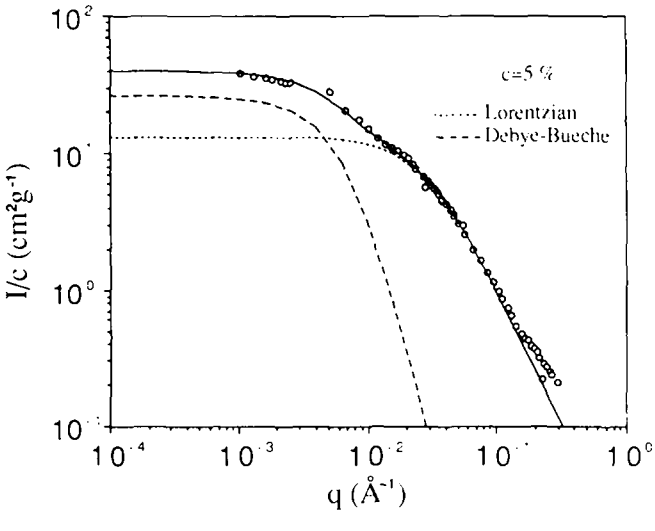

Figure 8 Reconstructed scattered intensity $I(q)$ obtained by adding the two contributions for a $c = 5\%$ solution. The dotted curve represents the Lorentzian behaviour with $\xi = 35$ Å (equation (15)), the broken curve is the contribution of the inhomogeneities (equation (21) with $a = 135$ Å) and the full curve is the total intensity (equation (19)). A satisfactory agreement with the experiments can be seen in the accessible range of q vectors

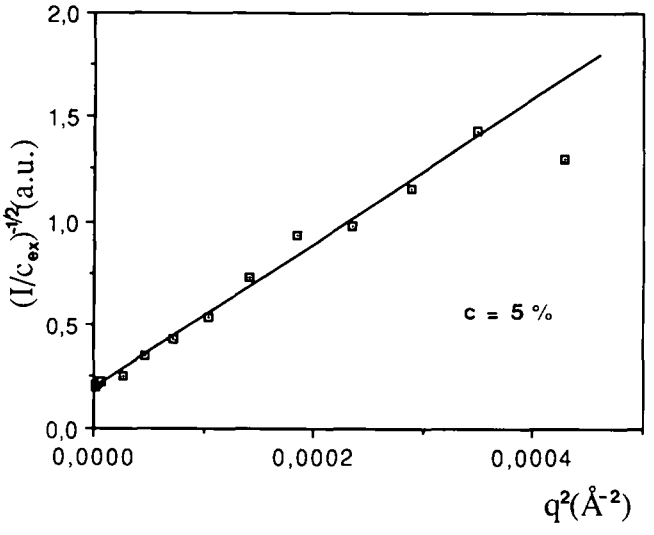

Figure 9 Excess scattering according to Debye Bueche model. A linear dependence for $I_{ex}(q)^{-1/2}$ *versus* q^2 is observed, whose slope gives the parameter a for $c = 5\%$

having an exponential decay over a typical length a:

$$\gamma(r) = \exp(-r/a) \tag{20}$$

The analytical expression $I_{ex}(q)$ of the scattering from inhomogeneities of a characteristic size a is given by the Fourier transform of equation (20):

$$I_{ex}(q) = \frac{I_{ex}(0)}{(1 + q^2a^2)^2} \tag{21}$$

We have subtracted from the total intensity $I(q)$ the Lorentzian component $I_{Lorentz}(q)$ and determined the excess scattering $I_{ex}(q)$. Then, by plotting $I_{ex}^{-1/2}(q)$ *versus* q^2, we have tested the validity of the scattering law given by equation (21), as is shown in *Figure 9*, for the 5% solution. Indeed, the characteristic sizes of the inhomogeneities deduced from the slope of $I_{ex}(q)^{-1/2}$ are $a = 220$ Å for the 2% solution and $a = 135$ Å for the 5% solution. These values are reasonably large compared to ξ ($\xi = 51$ Å and $\xi = 35$ Å respectively). The addition of the two components is shown in *Figure 8* for the 5% data.

DISCUSSION AND CONCLUSIONS

This investigation of the gelatin solutions leads to the following conclusions:

In the dilute regime, the chains are well dissolved. The model of a worm-like chain appears to describe correctly the chain conformation in dilute solutions; the persistence length of 20 Å indicates that the gelatin chains are less flexible than polystyrene, but much more than other biopolymers, like the polysaccharides, which are known to forms gels via a mechanism of helix formation (agarose).

The semi-dilute solutions exhibit scattering laws that do not agree with the universal picture of homogeneously entangled chains. LS and SANS measurements definitely reflect a departure from Lorentzian behaviour. The origin of these effects is not well understood, although they have been reported for other systems, like polystyrene in various solvents. For instance, for polystyrene in benzene (good solvent) or in cyclohexane (poor solvent) an excess scattering appears[31], which depends on the experimental conditions of preparation: upon centrifugation the excess scattering is attenuated, but an ageing effect appears when the sample is kept for a long time. It is not clear which preparation procedure leads to the equilibrium configuration of the solution. Gan *et al.*[33] working with atactic polystyrene in *p*-dioxane and in tetrahydrofuran (THF) noticed that the excess scattering is temperature-dependent. Measurements were totally reversible in heating and cooling cycles. Thus, at the moment there is no unanimous agreement about the origin of the excess scattering. In the first reference[31], the authors found that parameter a was larger than the radius of gyration of the dilute chains by a factor of 4, for low molecular weights (6×10^4 g mol^{-1}) and equal to R_g for high molecular weights (3×10^6 g mol^{-1}). Gan *et al.*[33] noticed that the length a decreased with concentration as c^{-1}.

In relation to the static measurements, we also performed dynamic LS experiments, which are reported in the accompanying paper[6]. These experiments corroborate the statement that the entangled gelatin solutions are not totally homogeneous. Indeed, the presence of a diffusive 'slow mode' was detected in the semi-dilute solutions, in addition to the fast diffusive mode, which is attributed to the cooperative movement of the chains ('pseudo-gel' behaviour). For gelatin solutions of concentrations varying from 1 to 20%, the diffusion coefficient of the slow mode decayed as the inverse of the macroscopic viscosity. This apparent Stokes-law behaviour enabled us to determine an equivalent hydrodynamic radius for the diffusing species, which is of the order of 750 Å.

The radius of gyration of the inhomogeneities, in the Debye–Bueche model, can be calculated: it differs from parameter a by a numerical factor. Indeed, the mean-square radius $\langle r^2 \rangle^{1/2}$ can be deduced from $\gamma(r)$ (equation (20)) by the usual statistical definitions[1,32]. We found:

$$\langle r^2 \rangle^{1/2} = \sqrt{12}\, a$$

For 2% and 5% solutions the radii of gyration of inhomogeneities would be respectively 760 Å and 460 Å. These values are comparable to those derived from dynamic LS, although some questions remain, such as the following.

(i) Inhomogeneities may have a distribution of sizes. Within the range of accessible scattering vectors, the static experiments are more likely to detect the smaller ones, while the temporal spectroscopic investigations are more sensitive to the slow movements due to the larger species. Thus, it would be interesting, for instance, to measure the scattering patterns at smaller q vectors ($\approx 10^{-4}$ Å^{-1}) in order to reach the Guinier range of the largest particles present in solution and to determine their radius of gyration.

(ii) Density contrast between inhomogeneities and the remaining solution is a crucial parameter in deriving their size. For increasing concentrations, we noticed that the parameter a of the Debye Bueche model decreased. Supposing that inhomogeneities have a dense core surrounded by an entangled envelope, we can imagine that the chain concentration in the outer part of the inhomogeneities is closer to the solution, for increasing amounts of gelatin. This concentration effect, then, leads to an apparent decrease in size of the objects and it could also imply that inhomogeneities have a complex specific structure.

(iii) One may question as well the validity of the

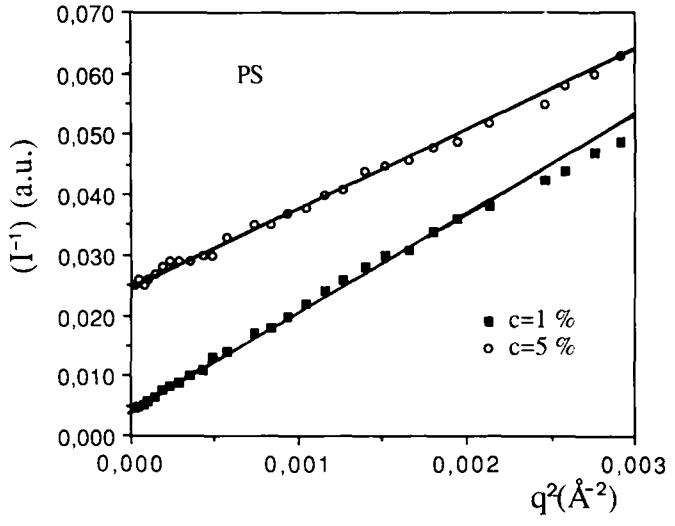

Figure 10 Scattering from semi-dilute solutions of deuterated polystyrene in CS_2. The polystyrene sample had a polydispersity index of 1.7 and an average molecular weight $M_w \sim 2.2 \times 10^5$ g mol^{-1}. The scattering curves have a Lorentzian shape, as shown from the linear dependence of $I^{-1}(q)$ *versus* q^2

theoretical model that we used to interpret LS and SANS measurements. Decomposition of the scattered intensity into two components, equations (15) and (21), first of all, supposes that the Lorentzian distribution with a *single* parameter ξ shoud be valid for an entangled solution of *polydisperse* chains. Therefore, in order to make a comparison with another system with approximately the same polydispersity index, we investigated a solution of deuterated polystyrene dissolved in CS_2 (good solvent). This sample was characterized by $M_w = 2.2 \times 10^5$ g mol^{-1} and a polydispersity index of 1.7. The results for SANS experiments are shown in *Figure 10* and they indeed display a simple Lorentzian shape. The ξ parameters deduced from the plots are $\xi = 55$ Å and $\xi = 22$ Å respectively for $c = 1\%$ and $c = 5\%$. These values are comparable to those of the gelatin sols. Secondly, the choice of the Debye Bueche model may not be unique; nevertheless it provides a correct order of magnitude for the size of the inhomogeneities and it fits the experimental data within the accessible range of q vectors.

Thus, we may conclude that both static and dynamic scattering experiments suggest that, in the standard conditions of preparation, the aqueous semi-dilute solutions contain inhomogeneities of the order of several hundred angstroms. More work is needed in order to elucidate the origin of these effects[6].

Another point that has been discussed in the literature is the possible relation between the excess small-angle scattering and the physical gelation ability of some polymeric solutions, like atactic polystyrene in a few selected solvents. Gan *et al.*[33] have noticed a relatively good correlation between gelation properties of these solutions, excess scattering and chain solvation: they suggested that formation of local 'crystals' or complexes between polymer and solvent was at the origin of the gelation process. In gelatin solutions, the mechanisms of gelation is now well accepted as being induced by the conformational change coil → helix, where the triple helices are stabilized by hydrogen bonds. The role of the solvent is important in the gelation mechanism[34], as water molecules participate in the formation of the junctions in which they are specifically oriented inside the triple helices. There is no evidence, however, from this investigation for a possible relation between the presence of a few inhomogeneities in the hot solution and the gelation ability of the gelatin solutions. A simple argument that one can give is that these domains are in any case in a small number (small volume fraction) and therefore they cannot drive the gelation mechanisms, which must involve the whole solution. They certainly represent a source of non-homogeneity of the gels as they form.

ACKNOWLEDGEMENTS

The authors are very much indebted to J. Teixeira for initiating the SANS investigation and for the numerous and stimulating discussions we have had while carrying out this project. It is a pleasure also to thank F. Schosseler, L. Leibler and M. Daoud for fruitful discussions, and J. Bastide and F. Boué for kindly providing us with the polystyrene sample and for their valuable suggestions and advice during this work. We express our gratitude to J. Lesec, who gave us access to the LS device that he developed. This research was partly supported by Sanofi-Bio-Industries.

REFERENCES

1 Glatter, O. and Kratky, O. 'Small-Angle X-ray Scattering', Academic Press, London, 1982
2 Daoud, M., Cotton, J. P., Farnoux, B., Jannink, G., Sarma, G., Benoit, H., Duplessix, R., Picot, C. and de Gennes, P. G. *Macromolecules* 1975, **8**, 604
3 Farnoux, B. *Ann. Phys.* 1976, **1**, 73
4 de Gennes, P. G. 'Scaling Concepts in Polymer Physics', 2nd Edn., Cornell University Press, Ithaca, NY, 1985
5 Boedtker, H. and Doty, P. *J. Chem. Phys.* 1954, **58**, 968
6 Herning, T., Djabourov, M., Leblond, J. and Takerkart, G. *Polymer* 1991, **32**, 3211
7 Djabourov, M., Leblond, J. and Papon, P. *J. Physique* 1988, **49**, 319, 333
8 Favard, P., Lechaire, J. P., Maillard, M., Favard, N., Djabourov, M. and Leblond, J. *Biol. Cell* 1989, **67**, 201
9 See for instance Chen, S. H. *Annu. Rev. Phys. Chem.* 1986, **37**, 351
10 Ward, A. G. and Courts, A. (Eds), 'The Science and Technology of Gelatin', Academic Press, London, 1977
11 Kuhn, W. *Kolloid Z.* 1934, **68**, 2
12 Deybe, P. J. *Phys. Colloid Chem.* 1947, **51**, 18
13 Rawiso, M., Duplessix, R. and Picot, C. *Macromolecules* 1987, **20**, 630
14 Kratky, O. and Porod, G. *Rec. Trav. Chim. Pays-Bas* 1949, **68**, 1106
15 Zimm, B. *J. Chem. Phys.* 1948, **16**, 1093
16 Oberthur, R. C. *Makromol. Chem.* 1978, **179**, 2693
17 Schulz, G. V. *Z. Phys. Chem. (B)* 1939, **43**, 25
18 Edwards, S. F. *Proc. Phys. Soc. London* 1966, **88**, 265
19 des Cloizeaux, J. *J. Physique* 1975, **36**, 281
20 Pezron, I., Herning, T., Djabourov, M. and Leblond, J. in 'Physical Networks' (Eds. W. Burchard and S. B. Ross-Murphy), Elsevier Applied Science, London, 1990, Ch. 18
21 Ise, N. *J. Chem. Phys.* 1962, **36**, 3248
22 Flory, P. 'Principles of Polymer Chemistry', Cornell University Press, Ithaca, NY, 1953
23 Gupta, A. K., Cotton, J. P., Marchal, E., Burchard, W. and Benoit, H. *Polymer* 1976, **17**, 363
24 Djabourov, M., Clark, A. H., Rowlands, D. W. and Ross-Murphy, S. B. *Macromolecules* 1989, **22**, 180
25 Clark, A. H. and Lee-Tuffnell, C. D. in 'Functional Properties of Food Macromolecules', Elsevier Applied Science, London, 1986, p. 203

26 Schaefer, D. W., Joanny, J. F. and Pincus, P. *Macromolecules* 1980, **13**, 1280
27 Schaefer, D. W. *Polymer* 1984, **25**, 387
28 Guenet, J. M., Willmott, N. F. F. and Ellsmore, P. A. *Polym. Commun.* 1983, **24**, 230
29 Dautzenberg, H. *J. Polym. Sci. (C)* 1972, **39**, 123
30 Okano, K., Wada, E., Kurita, K. and Fukuro, H. *J. Appl. Crystallogr.* 1978, **11**, 507
31 Kolberstein, J. T., Picot, C. and Benoit, H. *Polymer* 1985, **26**, 641
32 Debye, P. and Bueche, A. M. *J. Appl. Phys.* 1949, **20**, 518
33 Gan, J. Y. S., Francois, J. and Guenet, J. M. *Macromolecules* 1986, **19**, 173
34 Maquet, J., Theveneau, H., Djabourov, M., Leblond, J. and Papon, P. *Polymer* 1986, **27**, 1103